Effect of strain rate on constitutive properties for the shear failure of intact granite in seismogenic environments

Aitaro Kato,[1,2] Mitiyasu Ohnaka,[2,3] Shingo Yoshida,[2] and Hiromine Mochizuki[2]

Received 8 August 2003; revised 5 October 2003; accepted 9 October 2003; published 8 November 2003.

[1] To investigate how the constitutive parameters prescribing the slip-dependent law for the shear failure of intact rock are affected by strain rate, we conducted a series of triaxial fracture experiments at a strain rate in the range from 10^{-5} to 10^{-7}/s in seismogenic environments using Tsukuba granite samples. The experimental results showed that the peak shear strength decreases modestly with a reduction in strain rate, according to a logarithmic law. The reduction rate tested at wet conditions was larger than at dry conditions. It was found that the maximum slip-weakening rate slightly increases with an increase in strain rate at wet conditions. This indicates that the mechanical instability of the shear failure process is slightly enhanced by an increase in strain rate. *INDEX TERMS:* 5104 Physical Properties of Rocks: Fracture and flow; 5112 Physical Properties of Rocks: Microstructure; 7209 Seismology: Earthquake dynamics and mechanics. **Citation:** Kato, A., M. Ohnaka, S. Yoshida, and H. Mochizuki, Effect of strain rate on constitutive properties for the shear failure of intact granite in seismogenic environments, *Geophys. Res. Lett.*, *30*(21), 2108, doi:10.1029/2003GL018372, 2003.

1. Introduction

[2] The earthquake source at shallow crustal depths results from a shear rupture instability occurring on a pre-existing fault characterized by heterogeneities. This does not necessarily mean, however, that the earthquake source is a simple process of frictional slip failure on a pre-cut fault; indeed, there are increasing amounts of convincing evidence that the earthquake source is a mixed process between frictional slip failure on a pre-existing fault and the fracture of initially intact rock. It is, thus, critical to understand constitutive properties of the shear fracture of intact rock, and thereby to formulate the constitutive law as a unifying law that governs both frictional slip failure and shear fracture of intact rock [*Ohnaka*, 2003].

[3] The slip-dependent constitutive law for shear rupture is a unifying law that governs both frictional slip failure on a pre-existing fault and the shear fracture of intact rock [*Ohnaka*, 2003], and hence we assume a slip-dependent law as the constitutive law for the shear rupture including earthquake sources. In the framework of the slip-dependent constitutive formulation, *Kato et al.* [2003] demonstrated that constitutive properties for the shear failure of intact rock vary with depth in the brittle and brittle-plastic transition regimes. It has not been investigated, however, how constitutive properties of the shear failure of intact rock are affected by strain rate.

[4] Although much effort has been devoted to investigating the effect of strain rate on the shear fracture strength of intact rock at dry and room temperature conditions [*Masuda et al.*, 1988; *Lockner*, 1998], few attempt has been made to investigate how slip-dependent constitutive properties including the post-failure process depend on the rate of deformation in seismogenic environments [*Wong*, 1982]. *Lockner* [1998] deformed dry granite at two different strain rates of 10^{-5}/s and 10^{-7}/s; however, the constitutive relation obtained was for just before the onset of the localization of deformation. No systematic study on how the entire shear failure process, including the breakdown (or post-failure) process associated with the growth of macroscopic shear fractures in granite, is affected by strain rate in seismogenic environments has been done.

[5] The purpose of this paper is to investigate with laboratory experiments how the constitutive properties for the shear failure of intact granite are affected by the strain rate in seismogenic environments. In this paper, we will focus on the peak shear strength τ_p and the maximum slip-weakening rate $|d\tau/dD|_{max}$ to discuss how the constitutive property depends on the strain rate.

2. Experimental Method

[6] Tsukuba granite from the Ibaraki Prefecture in central Japan was chosen for this study. It is a homogeneous rock with a nearly isotropic fabric, and the grain size ranges from 0.2 mm to 1.3 mm (coarser than Westerly granite). This rock has commonly been used in previous studies, and its modal analysis has been given elsewhere [e.g., *Kato et al.*, 2003]. The blocks used for the present study had no visible meso-fabric structure, and samples were cored and deformed in the same direction. Circular-cylindrical test samples (40 mm long and 16 mm in diameter) were prepared with an accuracy of <0.02 mm. To drive away air trapped in interstitial pores of the rock samples, the samples were vacuum saturated with distilled water. Full water saturation was attained after 5 days of immersion. As pore pressure medium, the distilled water was used.

[7] The cylindrical granite sample was placed in a 2 mm-thick graphite sleeve of which strength is much lower than the granite. Since the graphite sleeve has a higher porosity, the sleeve was used to minimize any possible gradient in pore water pressure in the rock sample. The graphite sleeve also served as a buffer to prevent the silver jacket (a 0.3 mm-thickness tube covering the sample assembly and

[1]Institute for Frontier Research on Earth Evolution, Japan Marine Science and Technology Center, Yokosuka, Japan.
[2]Earthquake Prediction Research Center, Earthquake Research Institute, The University of Tokyo, Tokyo, Japan.
[3]Department of Earth Sciences, University College London, London, UK.

0094-8276/03/2003GL018372$05.00

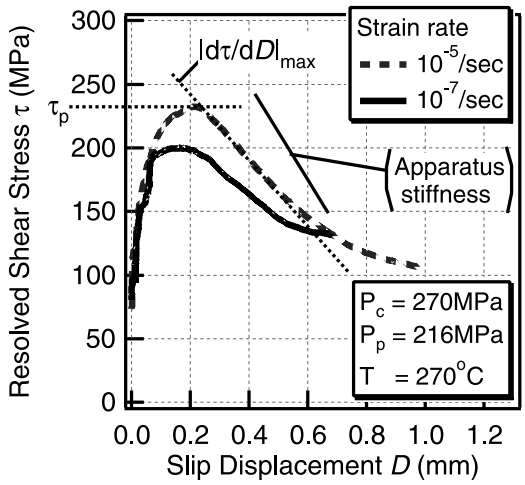

Figure 1. Constitutive relations observed under the condition (P_c, P_p, T) = (270 MPa, 216 MPa, 270°C) at the strain rate of 10^{-5}/s (broken curve) and 10^{-7}/s (solid curve). The stiffness (375 MPa/mm) of the loading system is also shown for comparison.

piston spacers) from rupturing. It was clearly demonstrated that dilatancy hardening is completely suppressed in the present experimental configuration, and the effective stress law holds for this Tsukuba granite even at a strain rate of 10^{-5}/s [*Kato et al.*, 2003].

[8] A triaxial testing apparatus used in the present experiments is designed for stabilizing the post-failure process by enhancing the stiffness of the loading system coupled to both high-response servo-hydraulics and digital control system. A detailed description of this apparatus and experimental configuration has been given in an earlier paper [*Ohnaka et al.*, 1997]. Both the confining pressure P_c and the pore water pressure P_p were servo-controlled to be constant. Temperature T was raised at a constant rate of 3°C/s to a pre-set value before axial load application. Experiments were performed at a strain rate in the range from 10^{-5}/s to 10^{-7}/s. To shorten the duration of the slowest experiment, the axial load was applied initially at the rate of 10^{-5}/s up to approximately a one-half level of the peak shear strength, and thereafter the load was applied at the rate of 10^{-7}/s up to the end of the run. This can be justified insofar as the elastic strain rate during the initial loading does not play a critical role in the eventual process of post-failure [*Lockner*, 1998].

[9] One run for the slowest experiments performed at a strain rate of 10^{-7}/s takes about 60 $\sim$ 90 hours, during which time the frictional force exerted by the loading piston may possibly be disturbed by temperature fluctuations in the pressure vessel. If this were to happen, it would be better to measure the axial load inside the pressure vessel to avoid such a disturbance. We therefore made an in-vessel measurement of the axial load in the slowest experiments, by mounting a pair of strain gauges on the silver jacket at a distance of 60 mm from the center of sample just outside of the heat insulator [see *Kato et al.*, 2003, Figure 1]. The strain gauges designed for strain-measurements at temperatures up to 250°C were used KYOWA-Dengyo. Temperature around the strain gauges was measured to be less than 150°C. The output of the internal load cell was calibrated against that of the external cell.

3. Experimental Results

3.1. Dependence of Constitutive Properties on Strain Rate

[10] The failure of intact rock occurs by shear faulting under compressive stress conditions. In order to obtain the constitutive relation for the shear failure, therefore, the failure strength has to be represented in terms of the resolved shear strength τ along the macroscopic fracture surfaces as a function of slip displacement D. The slip displacement is defined here as the relative displacement between both walls of the fault zone. The fault zone may include integrated amounts of slip associated with the deformation of asperities, micro-cracking and local displacement between contacting gouge fragments. Hence, both the shear strength and the slip displacement (corrected for the elastic displacement of the specimen) used for the constitutive formulation are defined in a macroscopic sense [*Ohnaka*, 2003].

[11] Figure 1 shows examples of the observed constitutive relations between τ and D tested at strain rates of 10^{-5}/s (broken curve) and 10^{-7}/s (solid curve), in which the constitutive relations at the two different strain rates are compared at the ambient condition (P_c, P_p, T) = (270 MPa, 216 MPa, 270°C). In this figure, τ_p is the peak shear strength, and $|d\tau/dD|_{max}$ is the maximum slip-weakening rate during the breakdown (or post-failure) process. Since the post-failure process is stabilized in the present experiments, note that the value of $|d\tau/dD|_{max}$ does not depend on the stiffness (375 MPa/mm) of the loading system (Figure 1). Note also that the stiffness of the loading system is not influenced by strain rate.

[12] It is found from Figure 1 that τ_p tested at the slowest rate of 10^{-7}/s is roughly 10% weaker than at the strain rate of 10^{-5}/s, and that $|d\tau/dD|_{max}$ tested at 10^{-7}/s is smaller than at 10^{-5}/s. This indicates that mechanical stability of the shear failure process is enhanced by a decrease in strain rate. We will discuss below in quantitative terms how the constitutive law parameters observed in the laboratory experiments vary with the strain rate at wet and dry conditions. The constitutive parameters evaluated in this study are listed in Table 1 with the experimental conditions. To check reproducibility, two duplicate runs were made at the strain rates of 10^{-5}/s, 10^{-6}/s, and 10^{-7}/s under the condition (P_c, P_p, T) = (270 MPa, 216 MPa, 270°C), and the results of these duplicate runs are compared in Table 1. The uncertainties of the parameters were ±3% for τ_p, and ±8% for $|d\tau/dD|_{max}$.

3.1.1. Peak Shear Strength τ_p

[13] To compare the dependence of τ_p on the strain rate, τ_p of intact granite at the strain rates of 10^{-5}/s and 10^{-7}/s is plotted as a function of the effective normal stress σ_n^{eff} in Figure 2, for data tested at wet conditions. Note that τ_p at the strain rate of 10^{-7}/s is lower than at 10^{-5}/s, and that the linear dependence of τ_p on σ_n^{eff} is also observed at the strain rate of 10^{-7}/s. The solid line in the figure shows the relationship between τ_p and σ_n^{eff} below 300°C at the strain rate of 10^{-5}/s calculated from the following equation [*Kato et al.*, 2003, equation 9]

$$\tau_p = C_{p0} + \mu_{p0}\sigma_n^{eff}, \quad (1)$$

Table 1. Laboratory Test Conditions and Constitutive Parameters Evaluated in the Present Study

Strain rate (1/s)	P_c (MPa)	P_p (MPa)	*Temp* (°C)	θ (deg)	τ_p (MPa)	$\lvert d\tau/dD\rvert_{max}$ (MPa/mm)
10^{-5}/s	270	216	270	29.6	232.4	262.0
"	"	"	"	27.5	237.1	285.0
3×10^{-6}/s	270	216	270	26.0	219.0	200.5
10^{-6}/s	270	216	270	28.0	215.6	167.0
"	"	"	"	25.0	212.7	260.4
10^{-7}/s	270	216	270	26.0	199.7	189.5
"	"	"	"	25.0	209.3	136.0
10^{-5}/s	378	216	270	27.5	341.5	270.7
10^{-7}/s	378	216	270	26.5	327.5	140.5
10^{-5}/s	460	216	270	29.5	413.0	89.8
10^{-7}/s	460	216	270	29.0	382.1	70.5
10^{-4}/s	100	dry	150	30.0	330.0	
10^{-5}/s	100	dry	150	28.5	323.3	
10^{-6}/s	100	dry	150	28.0	318.0	
10^{-4}/s	140	dry	210	29.0	366.0	286.0
10^{-5}/s	140	dry	210	29.5	350.2	210.0
10^{-6}/s	140	dry	210	29.0	343.0	272.0

P_c, confining pressure; P_p, pore water pressure; *Temp*, temperature; θ, failure angle; τ_p, peak shear strength; $\lvert d\tau/dD\rvert_{max}$, maximum slip-weakening rate.

where μ_{p0} is the internal frictional coefficient (0.7), and C_{p0} is the cohesive strength (108 MPa).

[14] Figure 3a shows a plot of τ_p against the logarithm of the strain rate $\dot{\varepsilon}$ for data tested at wet conditions, where τ_p has been normalized to the value at $\dot{\varepsilon} = 10^{-5}$/s for each condition. We find from this figure that τ_p decreases modestly with a logarithmic decrease in $\dot{\varepsilon}$, and that confining pressure does not significantly affect the dependence of τ_p on $\dot{\varepsilon}$ within the range of conditions tested. To quantify the effect of $\dot{\varepsilon}$ on τ_p, we assume that τ_p is a logarithmic function of $\dot{\varepsilon}$, and that the effect of $\dot{\varepsilon}$ is independent of temperature and effective normal stress σ_n^{eff} below 300°C. Under these assumptions, τ_p can be expressed in terms of σ_n^{eff}, and $\dot{\varepsilon}$ as follows

$$\tau_p = \left(C_{p0} + \mu_{p0}\sigma_n^{eff}\right)\left[1 + \xi \log\left(\frac{\dot{\varepsilon}}{\dot{\varepsilon}_0}\right)\right], \qquad (2)$$

where $\dot{\varepsilon}_0$ is the reference strain rate (10^{-5}/s), and ξ is a constant. The value for ξ can be evaluated by using the present set of data on τ_p, σ_n^{eff}, and $\dot{\varepsilon}$. The best-fit value of $\xi = 0.048 \pm 0.008$ was evaluated from an iterative least squares method. The broken line in Figure 3a denotes the relation between τ_p and $\dot{\varepsilon}$ determined from equation 2. Although the effect of $\dot{\varepsilon}$ on τ_p is logarithmic, τ_p has linear dependence on σ_n^{eff} below 300°C as shown in equation 2. This indicates that the effect of $\dot{\varepsilon}$ on τ_p is secondary compared with that of σ_n^{eff}.

[15] Figure 3b shows a plot of τ_p against the logarithm of $\dot{\varepsilon}$ for dry samples, where τ_p has been normalized to the value for τ_p at $\dot{\varepsilon} = 10^{-5}$/s. We notice from Figure 3b that τ_p for dry samples decreases modestly with a logarithmic decrease in $\dot{\varepsilon}$; however, the slope is lower than that at wet conditions. The best-fit value of $\xi = 0.025 \pm 0.01$ was evaluated, and this value is as small as a half of that at wet conditions (broken line). This is consistent with previous data of laboratory experiments at room temperature by *Lockner* [1998], who showed that the shear fracture strength of Westerly granite decreases by 2% per one order-of-magnitude decrease in the strain rate (Figure 3b). This indicates that the effect of $\dot{\varepsilon}$ on τ_p is larger at wet conditions than at dry conditions. This may be ascribed to the fact that the bond-breaking reaction is more enhanced by stress corrosion at wet conditions.

3.1.2. Maximum Slip Weakening Rate $|d\tau/dD|_{max}$

[16] The breakdown process becomes more stable as $|d\tau/dD|_{max}$ decreases. The parameter $|d\tau/dD|_{max}$ can thus be a measure of the stability or instability of the breakdown process. It is therefore important to investigate how $|d\tau/dD|_{max}$ depends on the strain rate. Figure 4a shows a plot of $|d\tau/dD|_{max}$ tested at wet conditions against the logarithm of

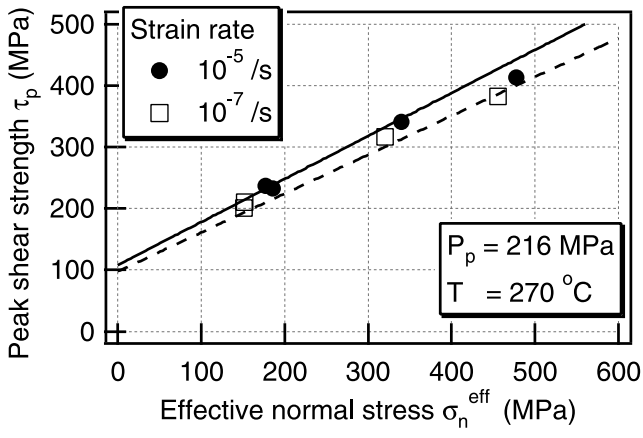

Figure 2. A plot of τ_p at the strain rates of 10^{-5}/s and 10^{-7}/s as a function of the effective normal stress σ_n^{eff} for the data tested at the conditions (P_c, P_p, T) = (270 ∼ 460 MPa, 216 MPa, 270°C). The solid line and the broken line denote the relations obtained from equation (2) at $\dot{\varepsilon} = 10^{-5}$/s, and 10^{-7}/s, respectively.

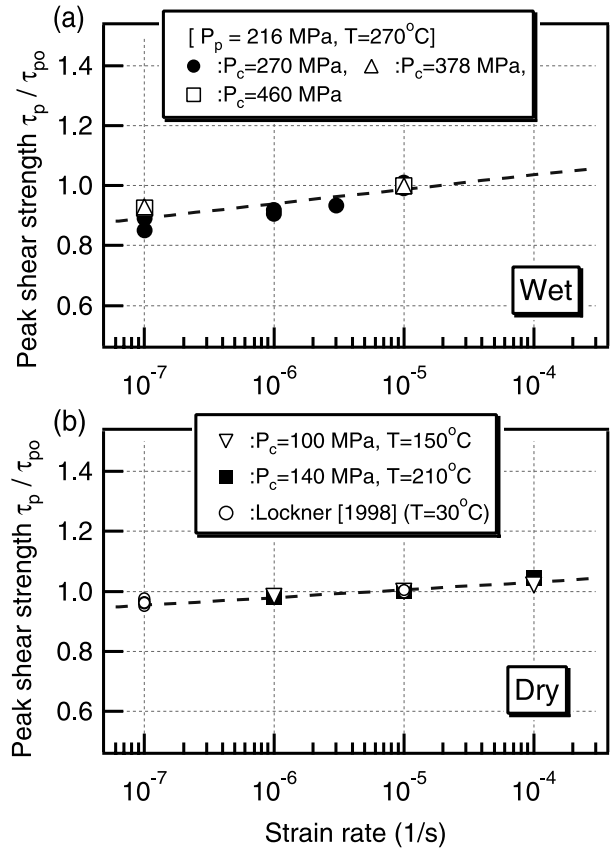

Figure 3. A plot of τ_p normalized to the value at $\dot{\varepsilon} = 10^{-5}$/s against strain rate $\dot{\varepsilon}$. (a) Wet samples; (b) Dry samples. The broken line is the fitted curve to the data points for the normalized τ_p, assuming that τ_p is a logarithmic function of $\dot{\varepsilon}$. Data from *Lockner* [1998] are also shown for comparison.

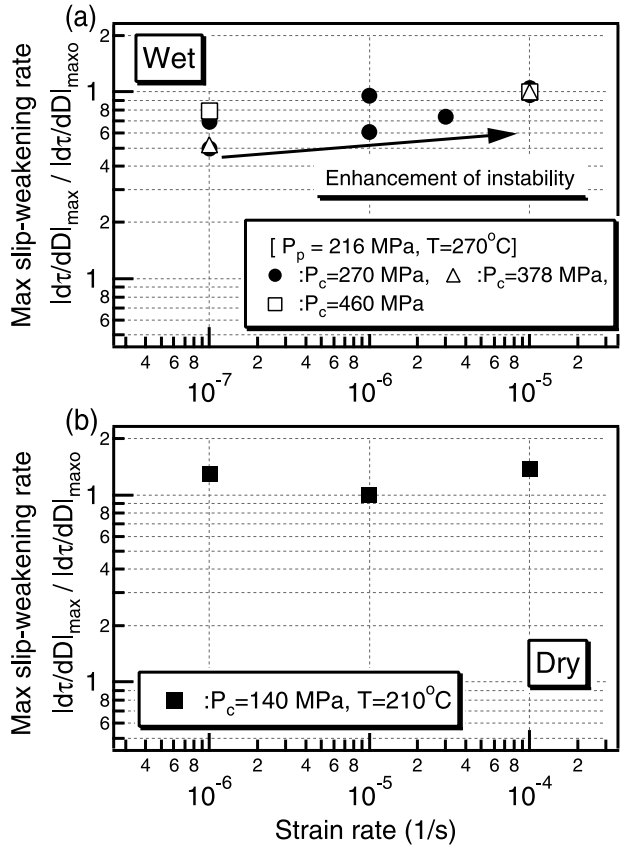

Figure 4. A plot of $|d\tau/dD|_{max}$ normalized to the value at $\dot{\varepsilon} = 10^{-5}$/s against strain rate $\dot{\varepsilon}$. (a) Wet samples; (b) Dry samples.

$\dot{\varepsilon}$, where $|d\tau/dD|_{max}$ tested at each condition has been normalized to the value at $\dot{\varepsilon} = 10^{-5}$/s. It is found from this figure that $|d\tau/dD|_{max}$ increases modestly with a logarithmic increase in $\dot{\varepsilon}$. This indicates that the mechanical instability of the shear failure process at wet conditions is slightly enhanced by an increase in $\dot{\varepsilon}$. In contrast, $|d\tau/dD|_{max}$ tested at dry conditions seems not to depend on $\dot{\varepsilon}$, and has roughly a constant value within the range in $\dot{\varepsilon}$ tested (Figure 4b). This suggests that the mechanical stability tested at dry conditions is not significantly affected by $\dot{\varepsilon}$.

4. Discussion

[17] Crack growth rate is enhanced at the crack tip in wet environments due to stress corrosion [e.g., *Atkinson*, 1984]. The present result that τ_p depends logarithmically on $\dot{\varepsilon}$ is consistent with that of subcritical crack growth by stress corrosion. Thus, we have assumed that the subcritical crack growth is the prime cause for the rate-dependence of τ_p tested in the present experiments.

[18] The effect of $\dot{\varepsilon}$ on τ_p can be rewritten equation 2 in terms of the natural logarithm of $\dot{\varepsilon}$ as $\xi\log(\dot{\varepsilon}/\dot{\varepsilon}_0) = \xi\log e \times \ln(\dot{\varepsilon}/\dot{\varepsilon}_0)$. We have $\xi\log e = 0.02 \pm 0.004$ from the substitution of 0.048 ± 0.008 for ξ. The value of $\xi = 0.02$ coincides with the value (of $0.012 \sim 0.026$) for the rate sensitivity of friction (this is what is called "direct effect" for the rate- and state-dependent formulation) obtained for wet granite gouges at temperatures from 250°C to 300°C [*Blanpied et al.*, 1995]. Further, *Marone* [1998] observed that the static frictional level decreased when samples were deformed at slower loading rates. This exactly agrees with the present result of the rate-dependence of τ_p. These results suggest that subcritical crack growth due to stress corrosion is the common mechanism occurring during deformation of intact rock and frictional sliding.

[19] The experimental fact that $|d\tau/dD|_{max}$ decreases with a decrease in $\dot{\varepsilon}$ at wet conditions means that the shear failure stability is enhanced as $\dot{\varepsilon}$ decreases. Although the operative mechanism for this is left for a future study, one possible mechanism may be physicochemical interaction between fresh fracture surfaces and water. This is suggested from the fact that the dependence of $|d\tau/dD|_{max}$ on $\dot{\varepsilon}$ was not significantly observed at dry conditions. A longer time is required for the physicochemical process at a slower strain rate, which may result in the enhancement of stability as $\dot{\varepsilon}$ decreases. The physicochemical mechanisms in hydrothermal environments may include dislocation glide [e.g., *Kato et al.*, 2003], solution-precipitation creep [e.g., *Blanpied et al.*, 1995], and/or growth of real contact area at asperity contact portions [*Dieterich and Kilgore*, 1994].

5. Conclusion

[20] We investigated with laboratory experiments how slip-dependent constitutive properties are affected by strain rate in seismogenic environments. The present results show that the relation between peak shear strength and strain rate obeys a logarithmic law, and that the effect in wet environments is greater than that in a dry environment. The maximum slip-weakening rate tested at wet conditions increases with an increase in strain rate. This indicates that the mechanical instability of the shear failure process is slightly enhanced with increasing strain rate.

[21] **Acknowledgments.** We are very grateful to two anonymous reviewers for their constructive comments and helpful suggestions, which led to substantial improvement in the original manuscript.

References

Atkinson, K. B., Subcritical crack growth in geological materials, *J. Geophys. Res.*, *89*, 4077–4114, 1984.

Blanpied, L. M., D. A. Lockner, and J. D. Byerlee, Frictional slip of granite at hydrothermal conditions, *J. Geophys. Res.*, *100*, 13,045–13,064, 1995.

Dieterich, J. H., and B. D. Kilgore, Direct observation of frictional contacts: New insights for state-dependent properties, *Pure Appl., Geophys.*, *143*, 283–302, 1994.

Kato, A., M. Ohnaka, and H. Mochizuki, Constitutive properties for the shear failure of intact granite in seismogenic environments, *J. Geophys. Res.*, *108*(B1), 2060, doi:10.1029/2001JB000791, 2003.

Lockner, D., A generalized law for brittle deformation of Westerly granite, *J. Geophys. Res.*, *103*, 5107–5123, 1998.

Marone, C., The effect of loading rate on static friction and the rate of fault healing during the earthquake cycle, *Nature*, *391*, 69–72, 1998.

Masuda, K., H. Mizutani, I. Yamada, and Y. Imanishi, Effects of water on time-dependent behavior of granite, *J. Phys. Earth*, *36*, 291–313, 1988.

Ohnaka, M., A constitutive scaling law and a unified comprehension for frictional slip failure, shear fracture of intact rock, and earthquake rupture, *J. Geophys. Res.*, *108*(B2), 2080, doi:10.1029/2000JB000123, 2003.

Ohnaka, M., M. Akatsu, H. Mochizuki, A. Odera, F. Tagashira, and Y. Yamamoto, A constitutive law for the shear failure of rock under lithospheric conditions, *Tectonophysics*, *277*, 1–27, 1997.

Wong, T.-F., Effects of temperature and pressure on failure and post-failure behavior of Westerly granite, *Mech. of Mat.*, *1*, 3–17, 1982.

A. Kato, Institute for Frontier Research on Earth Evolution, Japan Marine Science and Technology Center, Natsushima-cho 2-15, Yokosuka, 237-0061, Japan. (aitaro@jamstec.go.jp)

M. Ohnaka, S. Yoshida, and H. Mochizuki, Earthquake Prediction Research Center, Earthquake Research Institute, The University of Tokyo, Yayoi 1-1-1, Bunkyo-ku, Tokyo, 113-0032, Japan.